Improved Creep Strength and Creep Ductility of Type 347 Austenitic Stainless Steel through the Self-Healing Effect of Boron for Creep Cavitation

K. LAHA, J. KYONO, T. SASAKI, S. KISHIMOTO, and N. SHINYA

Composition of type 347 austenitic stainless steel was modified with the addition of boron and cerium. An improvement of creep strength coupled with creep ductility of the steel was observed with boron and cerium additions. The observation of enhanced precipitation of carbonitrides in boron-containing steel over that of boron-free steel may in part contribute to the increase in creep strength. Both grain boundary sliding and nucleation and growth of intergranular creep cavities were found to be suppressed in steel-containing boron. This results in an increase in creep strength and creep ductility. Auger electron spectroscopic analysis of the chemistry of creep cavity surfaces (exposed by breaking the creep-exposed steel specimen at liquid nitrogen temperature under impact loading) revealed the segregation of elemental boron on the creep cavity surface. Boron segregation, on the creep cavity surface in the absence of sulfur contamination, suppressed the cavity growth and provided the steel with a self-healing effect for creep cavitation. Cerium additions enabled boron to segregate on the cavity surface by effectively removing the traces of free sulfur in the matrix by the formation of ceriumoxysulfide (Ce_2O_2S).

I. INTRODUCTION

AUSTENITIC stainless steels such as types 316, 321, and 347 are widely used in power generating, petroleum, and chemical plants. However, in order to reduce environmental pollution, there is an urgent need to increase the thermal efficiency of such plants by increasing the working temperatures. Consequently, creep failure limits the life of these materials at these higher working temperatures. To that end, significant efforts have been undertaken to develop new creep resistance steels[1,2,3] as well as to increase the creep strength of existing steels.[4] The increase in creep strength of the existing steels has been accomplished through the optimization of elements present in the steels and also through the addition of minor elements. For example, Ti and Nb are added to austenitic stainless steels to increase their creep strength through the fine intragranular precipitation of Ti, Nb-carbonitride particles. However, the stability of such fine particles as well as the intergranular precipitation of brittle intermetallic phases such as σ and χ determine the long-term creep strength of such stabilized steels. Several investigations[2,5] have indicated an optimum level of Ti, Nb, C, and N contents in the austenitic stainless steels for higher long-term creep strength. This has been achieved by adjusting the Ti, Nb, C, and N contents with (Ti, Nb)/(C, N) ratio close to the stoichiometric value of the Ti, Nb-carbonitride precipitates; and also by ensuring that all the prior existing Ti, Nb-carbonitride particles dissolve during the solution annealing treatment of the steel so that they can reprecipitate as fine intragranular particles at dislocations during creep. In addition, a suggestion[6] also has been put forward to make the steel substoichiometric with respect to the carbonitride particles to increase its long-term creep strength through the "understabilizing" effect. These modifications have increased the long-term creep strength of austenitic stainless steels not only by imparting better stability to a higher density of carbonitride particles but also by delaying the extensive intergranular precipitation of brittle intermetallic phases such as σ and χ.[7] More recently, Cu has been added to austenitic stainless steels to increase their creep strengths by the intragranular precipitation of nanosize Cu particles.[4,8]

Creep failure proceeds with the nucleation, growth, and coalescence of grain boundary cavities. The evolution of grain boundary cavities during creep is closely connected to the physical properties of the cavity surface and the grain boundaries on which the cavities form.[9,10] Among the interfacial properties believed to strongly influence nucleation and growth of cavities are the energies of, and diffusivities along, both grain boundaries and cavity surface, as well as the resistance of grain boundaries to sliding.[11] These interfacial properties are in turn expected to be influenced by any trace element segregation that should take place.[12] The segregation of impurity elements such as O, S, As, and Sb on the grain boundary greatly lowers the interfacial energy of the boundary and enhances the creep cavitation.[13] These elements in solid solution, even in a minute quantity, must be controlled either by removing them during melting the steel or by alloying the steel with suitable elements so as to precipitate them out to increase the creep strength. Minor additions of rare earth elements such as Ce is found highly effective in removing O and S in the steel through the formation of ceriumoxysulfide (Ce_2O_2S).[14] Boron addition in high-temperature alloys has been reported to increase the creep strength, but the reason for its improvement is not completely understood.[15] In most instances, it is thought that the boron is concentrated on the grain boundaries where it enters into the precipitates and alters the character of the grain boundary/precipitates interface or matrix/precipitates

K. LAHA, Science Officer, is with the Mechanical Metallurgy Division, Indira Gandhi Centre for Atomic Research, Kalpakkam-603 102, Tamil Nadu, India. J. KYONO, Senior Engineer, T. SASAKI, Research Associate, S. KISHIMOTO, Senior Researcher, and N. SHINYA, Research Fellow, are with the Materials Engineering Laboratory, National Institute for Materials Science, Ibaraki 305-0047, Japan.

Manuscript submitted December 23, 2003.

on the grain boundary in such a way as to suppress microcavity formation.

In this study, the chemical composition of type 347 austenitic stainless steel was modified with the addition of minute amounts of boron and cerium with an aim to increase its long-term creep strength by suppressing creep cavitation. The evolution of grain boundary sliding and nucleation and growth of grain boundary cavities were studied to elucidate the beneficial effects of boron and cerium addition on the creep strength and creep ductility of the steel.

II. EXPERIMENTAL PROCEDURE

The chemical composition of standard type 347 austenitic stainless steel was modified with the additions of 0.07 wt pct of boron and 0.016 wt pct of cerium, and by the reduction of the Nb content from 0.8 wt pct with Nb/C ratio around 8 to 0.4 wt pct with Nb/(C + 6/7N) ratio around 3 and the sulfur content to the level of 0.002 wt pct. The steels were melted in vacuum arc furnaces at a vacuum level of 0.2 torr. The chemical compositions of the two steels designated as boron-free and boron-containing austenitic stainless steels are shown in Table I. The compositions were analyzed by chemical method. Each element was analyzed once using 3 grams of steel. The steel samples were subjected to a cold work of 36 pct reduction in diameter by swaging and were subsequently solution heat treated at different temperatures and for different times. The boron-free steel was solution heat treated at 1433 and 1473 K for 20 minutes followed by water quenching. The boron-containing steel was solution heat treated at 1433, 1453, and 1473 K for 20 minutes each and also at 1473 K for 8 minutes. The grain size of the steels was measured by the linear intersect method. Solution treatments of the boron-free steel at 1433 and 1473 K for 20 minutes resulted in average grain sizes of 47 and 80 μm, respectively. The grain sizes of the boron-containing steel solution heat treated at 1433, 1453, and 1473 K for 20 minutes were 45, 61, and 76 μm, respectively, and 64 μm for the solution heat treatment at 1473 K for 8 minutes. The addition of boron appears to have little effect on the grain size of the steel. Creep rupture tests were performed in air at 1023 K over a stress range of 47 to 118 MPa on both steels. The creep specimens were 10 mm in diameter and 72 mm in gage length. The temperature was controlled within $\pm$2 K over the entire gage length of the specimen during creep testing.

X-ray diffraction analysis of the precipitates in the steels after creep exposure was carried out. A solution of 10 pct acetyl acetate was used to electrolytically extract the precipitate from the steels. Limited transmission electron microscopy (TEM) investigations were carried out on the steels to determine the effect of boron addition on the precipitation. For this purpose, dice of 3 mm in diameter were machined from the creep-exposed specimen of the steels, reduced to 0.25-mm thickness by mechanical polishing under water, and finally thinned by double jet electropolishing using an electrolytic solution of 20 pct perchloric acid and 80 pct ethanol at 260 to 258 K, 20 V, and 0.1 A. The foils so prepared were examined in a JEOL* 2000 transmission electron microscope using an accelerating voltage of 200 kV.

*JEOL is a trademark of Japan Electron Optics Ltd., Tokyo.

Interrupted creep tests in an argon atmosphere were carried out on both of the steels, which were solution treated at 1433 K for 20 minutes, to study the effects of boron addition on grain boundary sliding, nucleation, and growth of grain boundary creep cavities. A 5-mm-diameter round specimen with two flat, parallel machined surfaces was used for this purpose. Details of the specimen are shown in Figure 1. The specimens were electropolished in a solution of 6 pct perchloric acid and 94 pct acetic acid at 20 V for 2 minutes to remove the work-hardened surface layer developed during machining the specimen. Microgrids and lines were inscribed on the flat surfaces of the specimen by focused ion beam (FIB) before creep testing. A gallium ion beam of 1 μm in diameter at an accelerating voltage of 20 kV and a current of 1.5 μA was used for this purpose. A section of the microgrid is shown in Figure 2. Creep tests performed at 1023 K and 78 MPa on such specimens of both steels were interrupted at predetermined intervals. The interrupted crept specimen surfaces were examined by scanning electron microscopy (SEM) to study the grain boundary sliding, nucleation, and growth of the creep cavities in the steels. The creep specimen was covered with a titanium foil to protect it from oxidization from the residual oxygen in the argon atmosphere during creep testing.

Chemistry of the creep cavity surface of both steels was examined by auger electron spectroscopy (AES). Notched specimens of 3 mm in diameter were machined from the

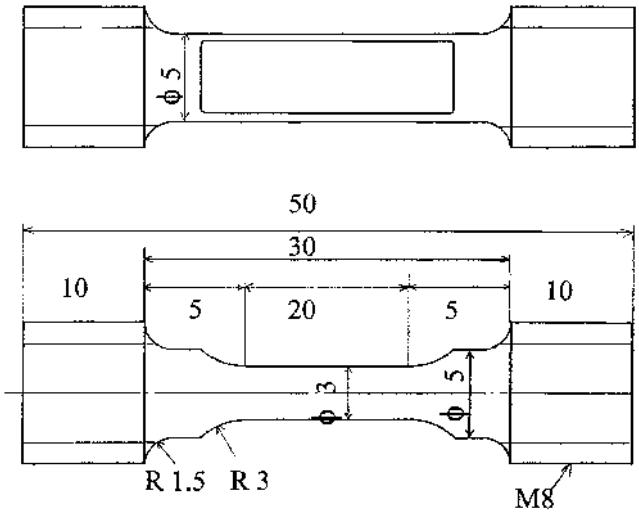

Fig. 1—Schematic diagram of the creep test specimen for microdeformation study (all dimensions are in millimeters).

Table I. Chemical Composition of the Melted Type 347 Austenitic Stainless Steels (Weight Percent)

Alloy	C	Si	Mn	P	S	Cr	Ni	Nb	N	B	Ce	Fe
Boron-free steel	0.080	0.59	1.68	0.001	0.002	17.96	12.04	0.41	0.077	—	—	balance
Boron-containing steel	0.078	0.68	1.67	0.001	0.002	18.15	11.90	0.38	0.072	0.069	0.016	balance

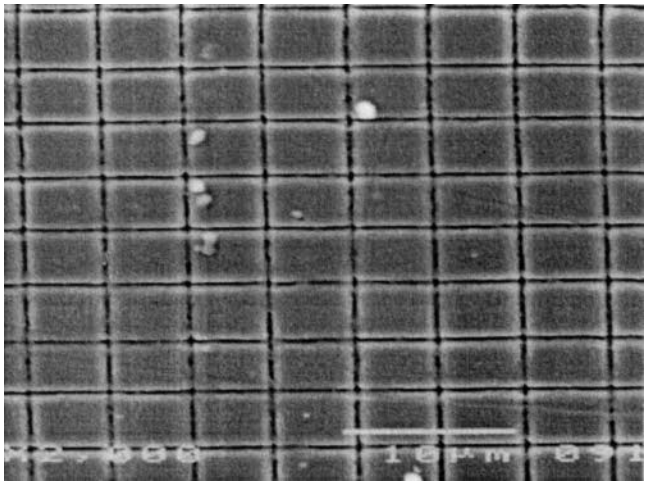

Fig. 2—A section of the microgrid inscribed on the flat surface of the creep test specimen by FIB.

precrept samples of the steels. The specimens were fractured under impact loading at liquid nitrogen temperature inside an AES chamber to expose the grain facets with creep cavities on them. Scanning auger analysis was performed using a PHI model 545 system. Auger spectra were taken at 10 keV with beam currents of up to 5 μA. The spatial resolution of this instrument was approximately 200 nm, which was adequate to confirm the intergranular nature of the fracture surface, as well as to identify individual creep cavities on the grain boundary facets.

III. RESULTS AND DISCUSSION

A. *Creep Strength and Microstructure*

Creep rupture tests were performed at 1023 K on the boron-free steel solution treated at 1473 K for 20 minutes and on the boron-containing steel at all the solution-treated conditions employed. The variation of the creep rupture life with applied stress of both steels, which were solution heat treated at 1473 K for 20 minutes, is shown in Figure 3. The addition of small amounts of boron and cerium had a remarkable effect on the creep rupture strength of the steel. The variation of creep strength with creep rupture life follows an equation of the type $\sigma = At_r^{-n}$, with $n = 0.18$ for boron-free steel and $n = 0.12$ for boron-containing steel. The value of n decreased with boron addition. The variations of creep rupture elongation percent and reduction in area percent with creep rupture life of both steels, which were solution treated at 1473 K for 20 minutes, are shown in Figures 4 and 5, respectively. The addition of boron and cerium increased the creep ductility of the steel along with creep strength, the effect of which was more pronounced at longer creep exposure time. Metallographic investigation of the creep-ruptured specimens revealed less creep cavitation in the boron-containing steel than that in the boron-free steel (Figure 6).

The effects of solution heat treatment on creep rupture strength and ductility of boron-containing steel are shown in Figures 7 and 8, respectively. The different solution heat treatments had no significant effect on the creep rupture strength of the steel. Ductility of the steel, especially at longer

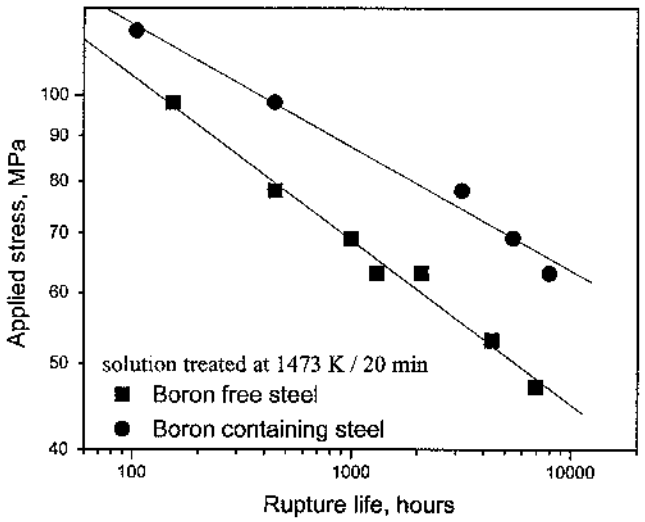

Fig. 3—Variation of creep rupture life of the steels with applied stress, solution treated at 1473 K for 20 min, and creep tested at 1023 K.

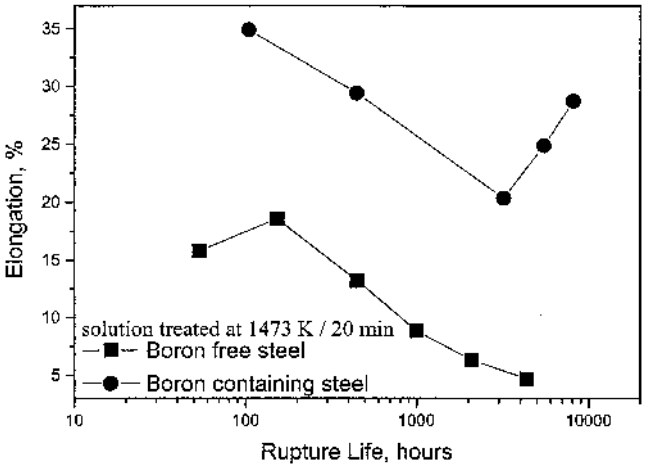

Fig. 4—Variation of creep rupture elongation percent with creep rupture life of the steels, solution heat treated at 1473 K for 20 min, and creep tested at 1023 K.

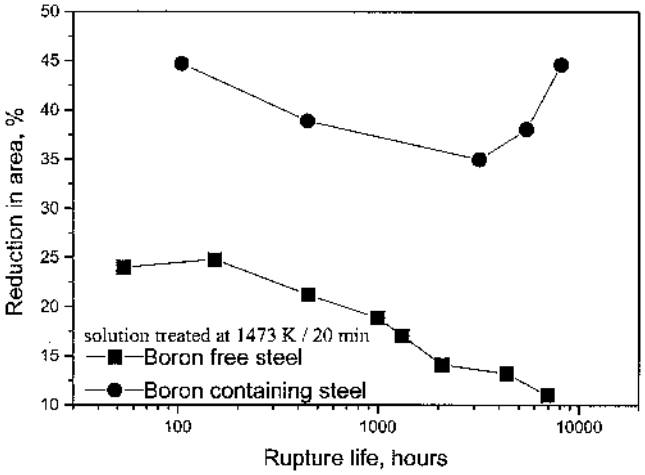

Fig. 5—Variation of creep rupture reduction in area percent with creep rupture life of the steels, solution heat treated at 1473 K for 20 min, and creep tested at 1023 K.

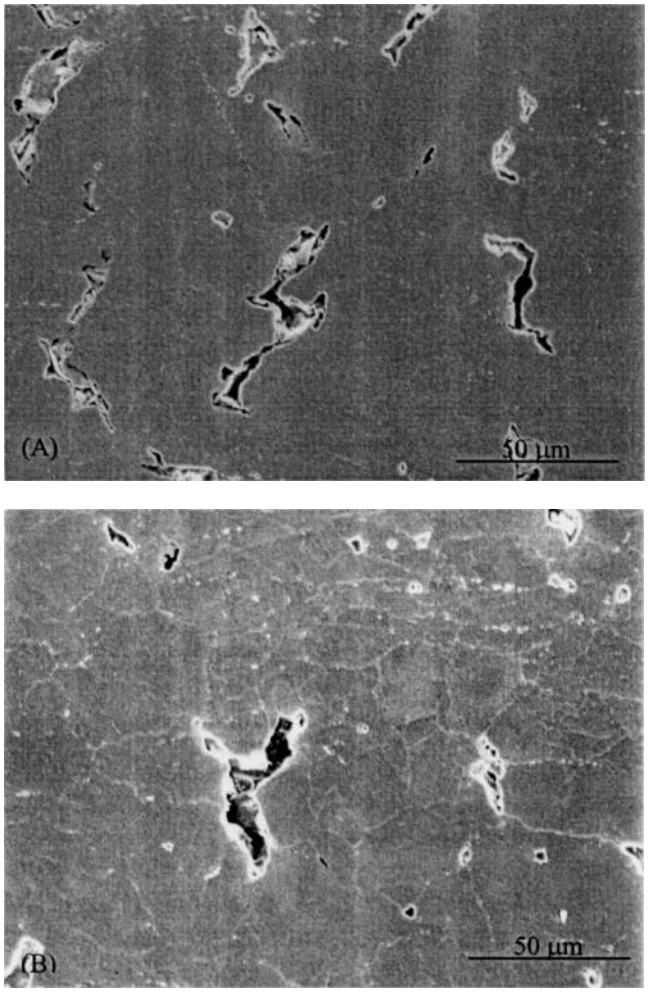

Fig. 6—SEM micrograph, showing creep cavitation in the steels after creep rupture test at 69 MPa: (*a*) boron-free steel (998 h) and (*b*) boron-containing steel (5461 h).

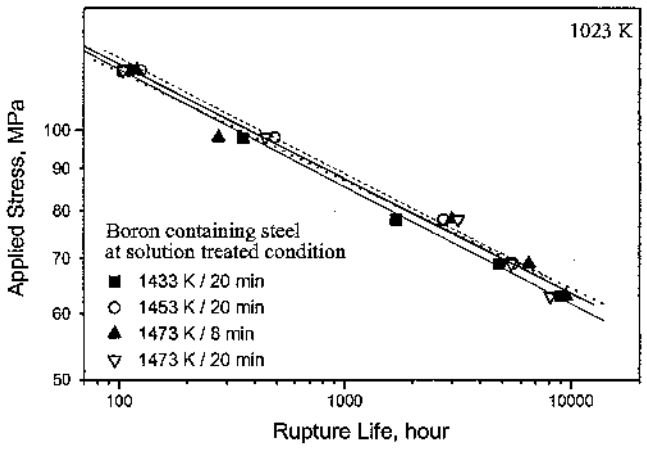

Fig. 7—Variation of creep rupture life with applied stress of boron-containing steel, showing the effect of solution heat treatment.

creep exposure, was slightly better for lower solution heat-treatment temperature. The grain size of the steel varied with the solution heat treatments in the range of 45 to 76 μm, being smaller at lower solution heat-treatment temperature.

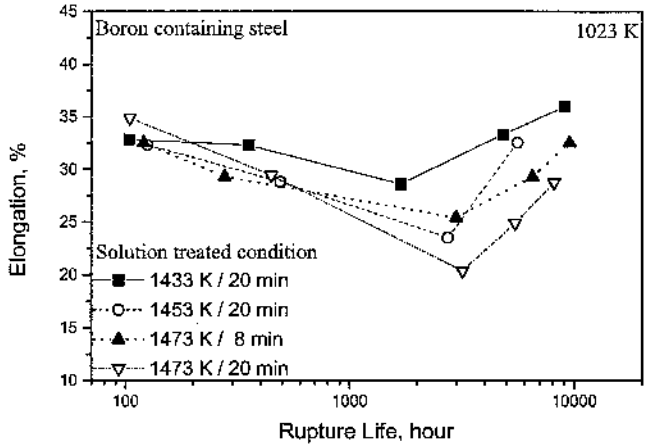

Fig. 8—Variation of creep rupture elongation percent with creep rupture life of the boron-containing steel, showing the effect of solution heat treatments.

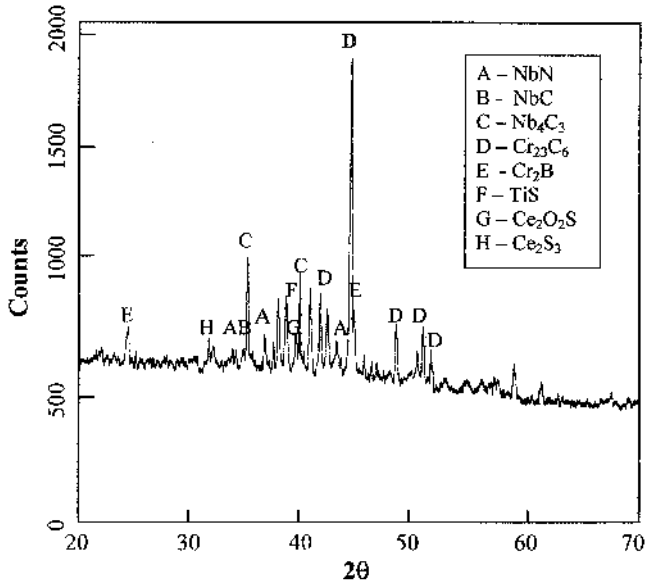

Fig. 9—X-ray diffraction analysis of the precipitates, extracted from the boron-containing steel, creep tested at 69 MPa, 1023 K, by electrochemical method.

The slight increase in ductility of the steel solution heat treated at lower temperature might be due its smaller grain size. A similar effect of solution heat treatment on creep rupture strength and ductility was reported by Teranishi *et al.*,[16] in a type 347 austenitic stainless steel containing no boron and cerium.

X-ray diffraction analysis of the precipitates in both of the steels after creep rupture at 1023 K and 69 MPa was carried out. Precipitate residues were extracted from the steels by the electrochemical method. Figure 9 indicates the presence of different precipitates in the boron-containing steel. In both steels, the presence of $Cr_{23}C_6$, Nb_4C_3, NbC, and NbN precipitates were observed. The observed carbonitride precipitation in both the steels was so reported by several investigators on the type 347 austenitic stainless steel.[7,17] X-ray investigations also indicated the presence of Ce_2S_3 and Ce_2O_2S precipitates in boron-containing steel, which also contained

cerium. Cerium has a strong affinity to both sulfur and oxygen and easily combines with them to form ceriumoxysulfide.[18] The addition of cerium in steel may be an effective way of removing traces of free sulfur and oxygen soluble in the steel. The beneficial effect of cerium addition on the creep rupture strength and ductility in a superalloy through control of the sulfur and oxygen contents in solid solution has been reported by Cosandey *et al*.[14] However, they have cautioned about the excess addition because of its embrittlement effect due to the precipitation of intergranular Ni_5Ce phase. Chromium-boride (Cr_2B) particles were observed in the boron-containing steel. The solid solubility of boron in a 18Cr-15Ni austenitic stainless steel has been reported to be about 90 ppm at 1273 K and the solubility boundary recedes rapidly with steel (Fig. 11), indicates high stability of the precipitates in the steel. The increase in amount of precipitation as well as the increased stability of the precipitates may be the reasons for increase in creep strength of the steel with boron addition (Figures 3 and 7). In a type 316 stainless steel, Fujiwara *et al*.[15] attributed the increase in creep strength as a result of boron addition to the enhanced precipitation of $M_{23}C_6$ carbides at dislocations.

The beneficial effect of boron addition on creep resistance of austenitic stainless steel is not completely understood. It has been attributed to the following: Boron addition enhances the precipitation of carbides through its effect on the solubility of both carbon and nitrogen; also, its addition somehow reduces the tendency of creep cavitation and hence increases the creep strength. Niobium-stabilized type 347 austenitic stainless steel, being highly prone to intergranular creep cavitations,[25] with an increase in its matrix strength through the enhanced precipitation due to boron addition is expected to be associated with the decrease in ductility. So the increase in strength coupled with an increase in creep ductility (Figures 3 through 5) in the steel indicates that the beneficial effect of boron addition on the creep rupture strength and creep ductility especially at longer creep exposure is not mainly due to the enhanced precipitation of carbonitrides and additional precipitation of boride (Figures 10 and 11).

B. *Grain Boundary Sliding*

In order to have a better insight as to why creep strength and creep ductility increased with the addition of boron and

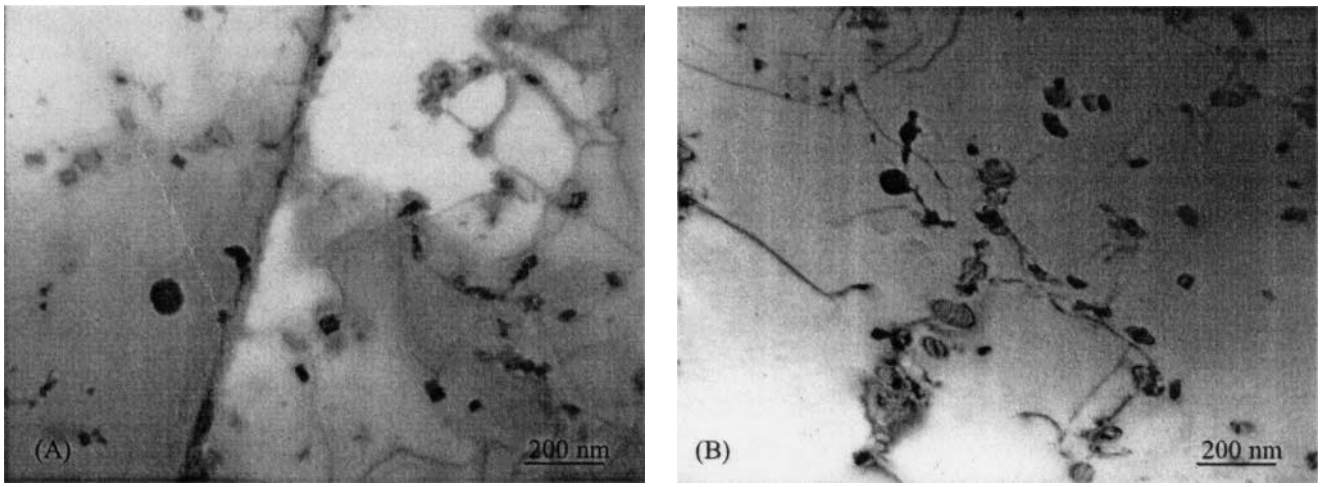

Fig. 10—Typical TEM micrographs of the boron-free steel after creep exposure at 1023 K for (*a*) 78 MPa, 447 h; and (*b*) 47 MPa, 6950 h.

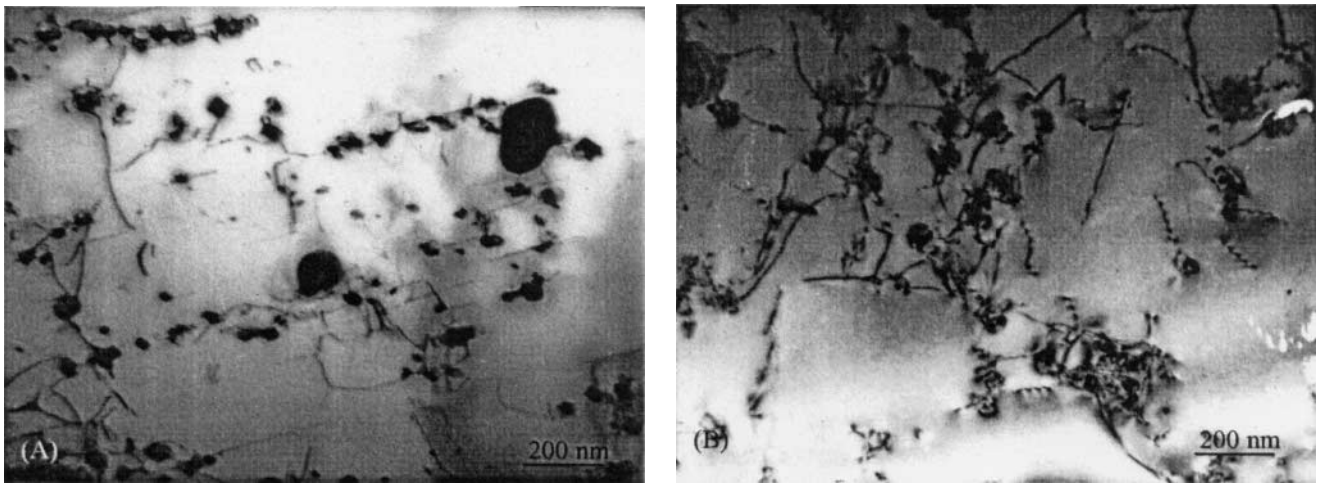

Fig. 11—Typical TEM micrographs of the boron-containing steel after creep exposure at 1023 K for (*a*) 98 MPa, 446 h; and (*b*) 63 MPa, 8876 h.

cerium in the steel, investigations were carried out on grain boundary sliding, nucleation, and growth of grain boundary creep cavities on both of the steels solution heat treated at 1433 K for 20 minutes. For this purpose, microgrids and lines were inscribed on the polished surface of the creep specimens by FIB (Figure 2). Creep tests were performed at 78 MPa and 1023 K on such specimens of the steels in an argon atmosphere and interrupted at some predetermined intervals. Polished surfaces of the interrupted creep specimens of both the steels were examined employing SEM to study the grain boundary sliding and grain boundary creep cavity nucleation and growth. Figure 12 shows the SEM micrograph of the boron-containing steel illustrating the different effects such as grain boundary sliding, grain rotation, nucleation and growth of grain boundary cavities, and their interlinkage on creep exposure. The schematic representation of grain boundary sliding on creep exposure is shown in Figure 13. The grain boundary displacements both along the longitudinal (u_y) and transverse (u_x) to the applied stress direction were measured by the offset of the microgrid lines across the grain boundary on creep exposure; whereas optical interferometry was used to measure the grain boundary displacement perpendicular to the specimen's surface (u_z). The offsets of the interference fringes shown in Figure 14 were caused by the grain boundary displacement perpendicular to the specimen's surface. However, soon it was realized that grain offsets of more than 0.2 μm were not possible to measure by this method because the wavelength of the light used for the measurement was 0.6 μm and also because the particles in the steels made the measurement difficult. A similar view was also expressed by Kishimoto *et al.*,[26] on their measurement of grain boundary sliding in a type 321 austenitic stainless steel. So the measurement of grain offset perpendicular to the specimen's surface (u_z) was abandoned. Figure 15 shows

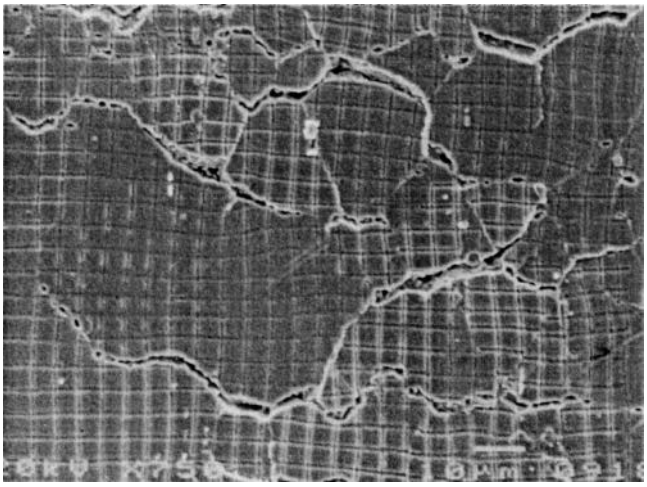

Fig. 12—SEM micrograph illustrating the different deformation and cavitation effects on creep exposure for 1200 h at 1023 K, 78 MPa in the boron-containing steel.

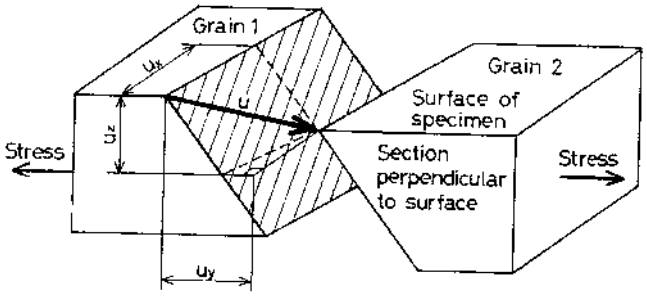

Fig. 13—Schematic representation of grain boundary sliding on creep exposure.

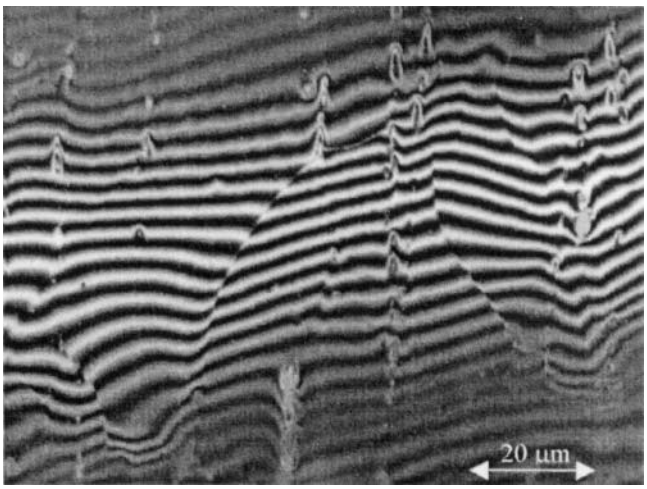

Fig. 14—Micrograph showing the offset of optical interference fringes caused by grain boundary displacement perpendicular to the specimen's surface (u_z) on creep exposure for 50 h at 78 MPa and 1023 K in boron-free steel.

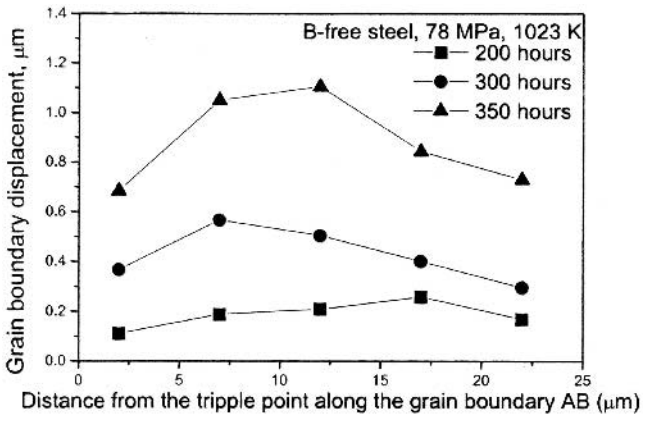

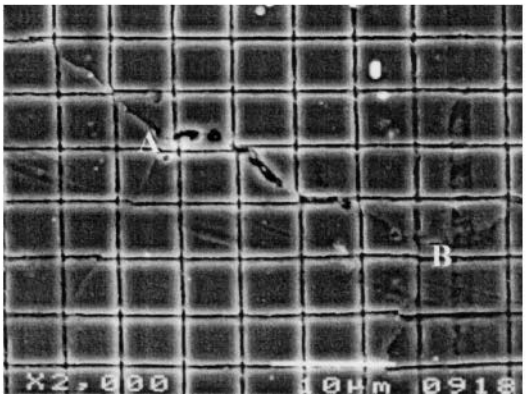

Fig. 15—Variation of grain boundary displacement (u_x) across the grain boundary *AB* in the transverse direction of applied stress after different creep exposures at 78 MPa and 1023 K in the boron-free steel.

the variation of the grain boundary displacement across the grain boundary AB, in the transverse direction of applied stress after different creep exposures. The displacements were measured by the offset of the longitudinal (with respect to stress direction) lines of the grid intersecting the grain boundary AB. The offsets were measured by optical traveling microscope from the SEM images of the microgrid on the specimen surface. The displacement was not uniform along the length of the grain boundary and decreased on approaching the grain boundary triple points. This suggests that grain boundary sliding was a heterogeneous process. The heterogeneity in matrix deformation (difference in the density of grain boundary particles and ledges) and grain boundary structure along the grain boundary may be some of the factors responsible for the heterogeneous grain boundary sliding. Nucleation and growth of creep cavities on the boundary complicates the grain boundary sliding process.

The longitudinal strain due to grain boundary sliding was calculated by dividing the mean offsets of the transverse lines (with respect to stress direction) of the grid intersecting a grain boundary by the projected length of the grain boundary in the longitudinal direction. The measurements were carried out at several grain boundaries to arrive at the mean value. Figure 16 shows the variations of total creep strain as well as strain due to grain boundary sliding with creep exposure time for both the steels. The secondary creep rate was found to decrease with boron addition (Figure 16). Enhanced precipitation of carbonitrides in the steel with the presence of boron (Figures 10 and Fig. 11) as well as the precipitation of boride is expected to decrease the creep rate. Grain boundary sliding was also greatly suppressed with the addition of boron (Figure 16). The contribution of grain boundary sliding strain to total creep strain was much more in boron-free steel than that in boron-containing steel. The reason for the strengthening of grain boundary and hence the sliding resistance is not precisely known. The solid solubility of boron in austenitic stainless steel is very low and has a strong tendency to segregate to the grain boundaries. This segregation tendency is a result of the large misfit of boron atoms in both substitutional and interstitial sites of the austenitic lattice.[27] Boron has a relatively high melting point of approximately 2303 K. Its segregation on the grain boundary is expected to reduce the grain boundary diffusivity and hence increases the grain boundary sliding resistance. Also, considering the low solubility of boron and its strong tendency to grain boundary segregation, it is possible that boron affects the precipitation behavior at the grain boundaries[27] as well as increasing the grain boundary sliding resistance.

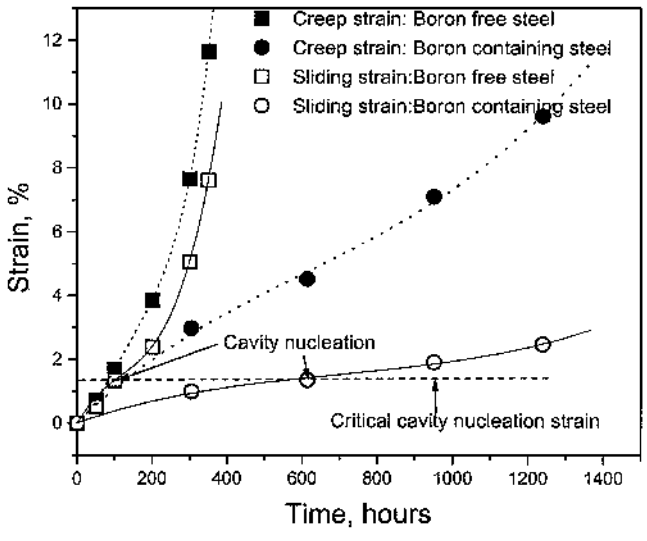

Fig. 16—Variation of total creep strain as well as strain due to grain boundary sliding with creep exposure at 78 MPa and 1023 K for both the steels.

C. *Creep Cavitation*

Grain boundary creep cavitations of *r* type were observed in both steels (more extensively in the boron-free steel). Creep cavitations are commonly categorized as *r* type (round) and *w* type (wedge).[28] The *r*-type cavitations are associated with the nucleation of creep cavities at the irregularities on the grain boundary such as ledges resulting from the impingement of slip planes on grain boundary, cusps resulting from the intersection of sub-boundaries with grain boundaries, grain boundary particles, *etc*., whereas the *w*-type cavitations are associated with the nucleation and growth of cracks at the junction of grain boundaries. The *r*-type cavitations observed in both steels are shown in Figure 17. Cavities were found to nucleate even at the termination points of the slip lines to the particles on the grain boundaries (Figure 17(b)) as well as on the twin boundaries (Figure 17(c)). The nucleation of creep cavities was followed by relatively more extensive grain deformation, as revealed by the formation of slip lines in boron-containing steel as compared to that in boron-free steel (Figures 17(a) and (b)). Nucleation of *r*-type cavities in a type 347 austenitic stainless steel was also reported by Needham and Gladman.[25] If the stress concentrations, produced when sliding is held up by a finite amount of material, are not relaxed, then cracks nucleate at the irregularities on the grain boundary. Smith and Barnby[29] showed that for grain boundary particles $2c$ in diameter and distance $2d$ apart, the nucleation stress is given by

$$\tau = (\pi/2)(c/d)^{1/2}(4\gamma G/(1-\nu)d))^{1/2} \quad \text{for } c \ll d \quad [1]$$

where γ is the grain boundary surface energy, G is the shear modulus, and ν is Poisson's ratio.

From Eq. [1], the stress to nucleate a cavity is expected to increase (or the nucleation of cavities will be delayed) if the distance between particles is sufficiently small or the interfacial energy sufficiently high. Since boron addition is believed to increase the grain boundary precipitation and also improve the bonding between the matrix and precipitates, it is expected that its addition will increase the stress required to nucleate the creep cavity. The strains for nucleation of creep cavities are indicated in Figure 16 for both steels. It appears that there is a critical strain for the nucleation of creep cavities that is independent of boron addition, signifying that the bonding of the precipitate with the matrix might not have appreciably changed with the addition of boron. Since the critical strain was achieved earlier in boron-free steel due to its decreased sliding resistance, creep cavity nucleation occurred much earlier than that in boron-containing steel. Variation of the number of cavities per unit volume with creep exposure time is shown in Figure 18. The number of cavities per unit volume N_v was derived from[25]

$$N_v = 2n_a m/\pi \quad [2]$$

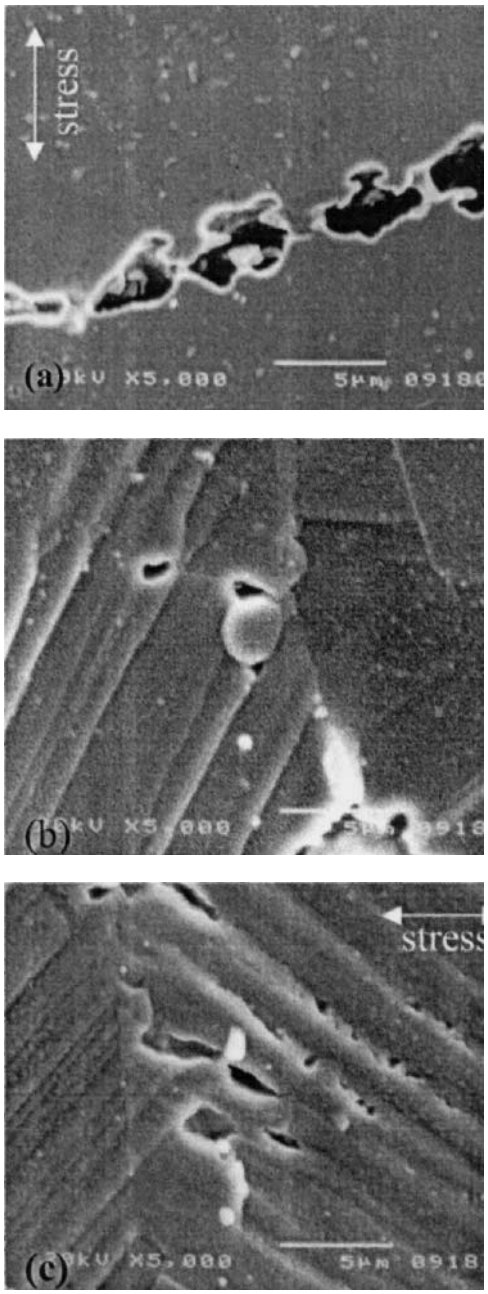

Fig. 17—Creep cavitation (78 MPa and 1023 K): (*a*) in boron-free steel after 300 h; (*b*) and (*c*) boron-containing steel after 1200 hours, cavitation at the intersection point of slip line with particle and at twin boundary, respectively.

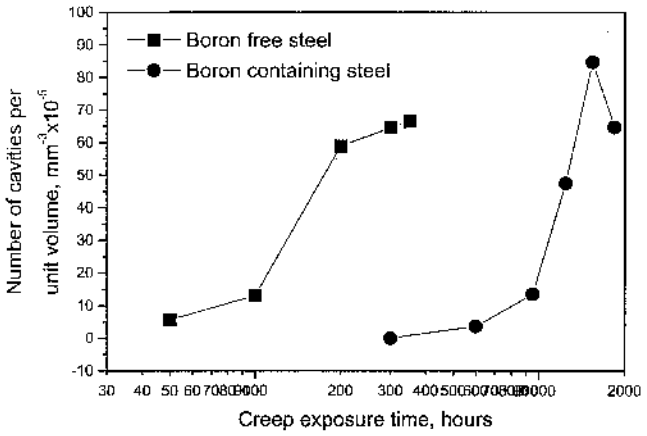

Fig. 18—Variation of number of cavities per unit volume (no./mm^3) with creep exposure at 78 MPa and 1023 K for both the steels.

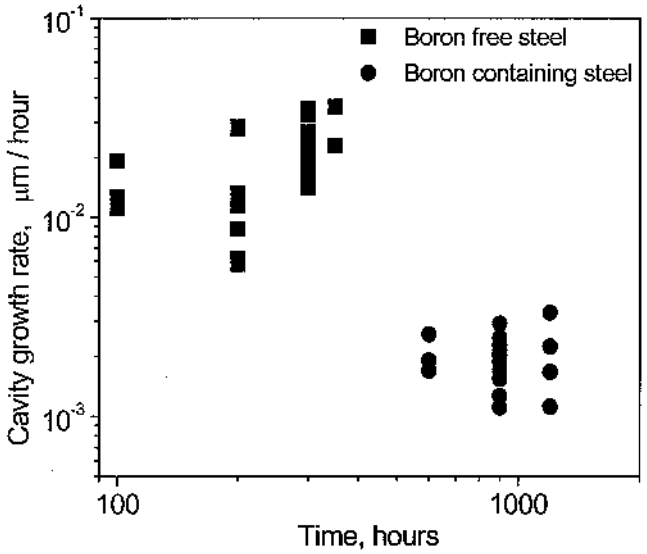

Fig. 19—Variation of cavity growth rate with creep exposure at 78 MPa, 1023 K for both the steels.

where n_a is the number of cavities per unit area of the plane section and m is the mean reciprocal of the apparent diameter of the cavities in the plane section. In both steels, cavity nucleation occurred throughout the creep exposure once the critical strain for nucleation was achieved. The addition of boron in the steel delayed the nucleation of creep cavities. In a type 347 steel, Needham and Gladman[25] reported a continuous nucleation of creep cavity with creep exposure and the nucleation were controlled by creep deformation process.

Figure 19 compares the growth rate of creep cavities at 78 MPa and 1023 K in both steels. Individual cavity dimensions were measured on interruption of the creep test employing SEM and optical traveling microscopy. The average growth rate of the cavity for the interval was calculated. Measurements were carried out on several cavities until they formed a coalescence with each others. Boron addition in the steel decreased the cavity growth rate by approximately an order of magnitude. Figure 20 compares the fractional length of the cavitated grain boundary of the steel. The total length of the cavitated grain boundary was calculated as[21]

$$L = n_a C_{av} \qquad [3]$$

where C_{av} is the average length of the cavity.

The number of grains in a plane section was calculated by considering the grain as spherical in shape with an average diameter of 50 μm. The total length of grain boundary in the plane section was calculated accordingly. It should mentioned that the interrupted creep tests to study creep cavitations were carried out on both steels solution heat treated at 1433 K for 20 minutes. The heat treatment resulted in average grain sizes of 47 and 45 μm, respectively, in the

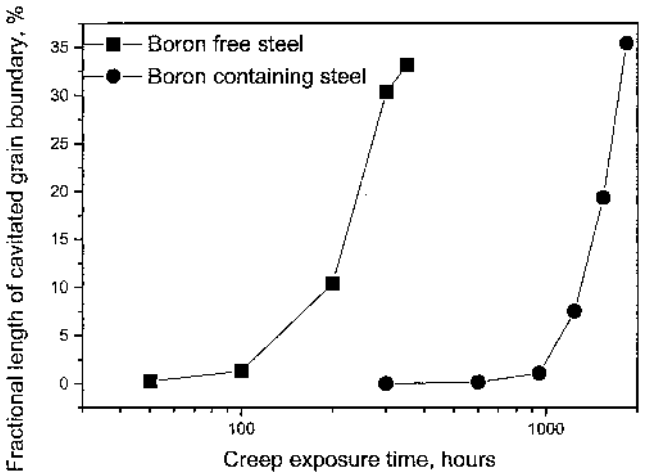

Fig. 20—Variation of the fractional length of cavitated grain boundary with creep exposure at 78 MPa and 1023 K for both the steels.

boron-free and boron-containing steels. An average grain size of 50 μm for both steels was taken for the calculation of grain boundary length. Boron addition in type 347 austenitic stainless steel delayed the nucleation of creep cavity, and suppressed the growth rate of the nucleated cavities, resulting in the increase in both creep strength and ductility (Figures 3 through 5).

The conclusions regarding the effect of boron addition on the nucleation and growth of creep cavities in the steel were based on the observations made on the cavities nucleated on the surface of the creep specimens. It should be noted that in stabilized austenitic stainless steels, Tanaka *et al.*[31] reported the predominate creep cavitation on the surface of the specimen rather than on those in the interior. Predominant surface cavitations were also observed in both the steels investigated. However, even then, the conclusions based on the observations made on the surface cavitations that the boron addition retards the creep cavitations in the steel are expected to hold good for cavitations inside the specimen.

D. *Segregation Effect on Cavity Surface*

Boron addition along with cerium was found to increase both the creep strength and creep ductility of the steel (Figures 3 through 5). The increase in creep deformation and grain boundary sliding resistances of the steel with the addition of boron, because of the enhanced precipitation of carbonitrides as well as the boride precipitation, could increase creep strength and creep ductility of the steel. It is to be noted that the ductility of the boron-containing steel increased further at longer creep exposures (Figures 4 through 8), which is in contradiction to the usual observation that ductility decreases with an increase in rupture life. With no further precipitation in the steel on longer creep exposures (Figure 11), the increase in ductility could not be accounted for by the increase in deformation and grain boundary sliding resistances. This increase in creep ductility at longer creep exposure appears to be related to the growth of creep cavities.

Nucleation of creep cavity was delayed in the steel-containing boron, but once the critical strain for cavity nucleation was achieved, the cavity nucleation rates were equal to those in the boron-free steel (Figure 18). The cavity growth rate in the steel was found to be suppressed with the boron addition. Growth of boundary cavities during creep is closely connected to the physical properties of the cavity surfaces and the grain boundaries on which the cavities form. Under stress, atoms at the cavity surface diffuse along the cavity surface and deposit on the grain boundary to grow the cavity. The creep cavity growth rate is expected to be strongly affected by the energies of the grain boundary and cavity surface and also by the diffusivity along both the grain boundary as well as cavity surface.[9] These interfacial properties are in turn expected to be influenced by any trace element segregation that could take place during creep.[32] White *et al.*[33] in their study on sulfur and phosphorus affecting creep cavitation in a 304 austenitic stainless steel reported sulfur concentration on a cavity surface approximately 10^3 times that in the bulk. Even a trace amount of bulk sulfur content can contaminate the cavity surface. Sulfur segregation on cavity surface decreases the surface energy and accelerates the cavity nucleation and growth. Also, segregated sulfur increases the diffusivities along both the grain boundary and cavity surface, and thus accelerates the creep cavity growth rate.[34] Relatively lower creep strength with low creep ductility in boron-free steel (Figures 3 through 5) might be due to the accelerated creep cavitation (Figures. 18 through 20). This can be accounted for by the segregation of sulfur on the cavity surface, which will be discussed in the next paragraph.

The chemistry of the creep cavity surface was examined by AES in both steels after creep testing at 69 MPa and 1023 K. The creep-exposed specimens of the steels were fractured by impact loading at liquid nitrogen temperature in the AES chamber to expose the creep cavity surface. Figure 21 shows the fracture surfaces of both steels containing creep cavities on grain boundary, indicating that this procedure was effective in exposing the cavity surface. The AES is sensitive to only the top few atom layers on a fracture surface, making it a useful technique for studying any trace element segregation that might have occurred. Auger spectra were obtained from several creep cavity surfaces in Figures 21(a) and (b). Only relevant portions of the auger spectra (*i.e.*, region containing C, B, S, Cr, Fe, and Ni peaks) were obtained in order to minimize the data acquisition time required for reasonable signal-to-noise ratios. Typical auger spectra obtained from cavity surface of the steels are shown in Figures 22 and 23, respectively, for the boron-free and boron-containing steels. The presence of sulfur segregation was observed on the creep cavity surface of boron-free steel, whereas no such segregation was observed in boron-containing steel. Boron-containing steel had also a minute amount of cerium. Cerium has a strong affinity to sulfur and oxygen and the presence of ceriumoxysulfide (Ce_2O_2S) in the precipitate residue (Fig. 9) indicates that cerium addition was highly effective in removing the traces of soluble sulfur in the matrix. In the absence of sulfur contamination on the nucleated cavity surface, boron was found to have segregated on it during creep testing in the boron-containing steel, which is evident from the auger spectra (Figure 23). The energy position and shape of the boron peak indicate that the boron was in elemental form.[35] In boron-containing steel, in the absence of sulfur contamination, most of the nucleated cavity surfaces were expected to be covered with a filmy segregation of elemental boron. Boron segregation is expected to decrease the diffusivity along the cavity surface

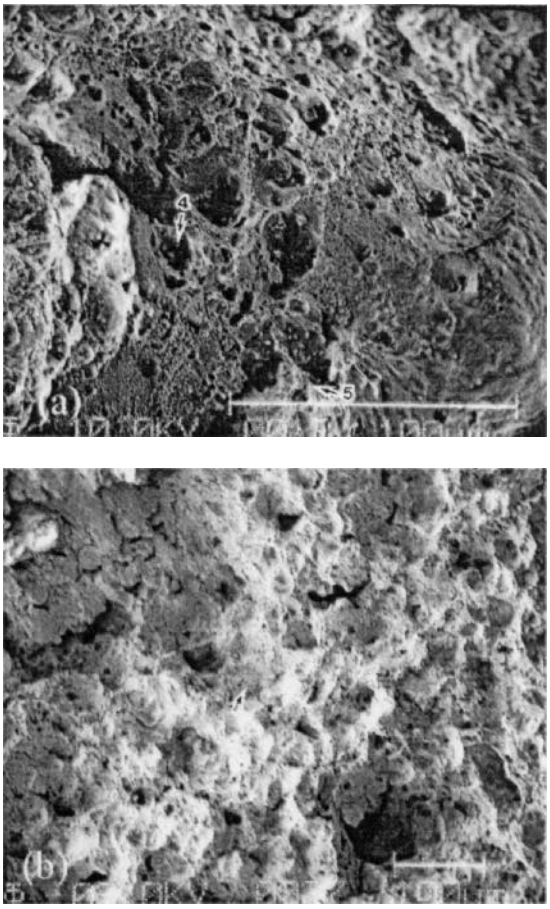

Fig. 21—SEM micrograph showing creep cavity surface, exposed by breaking at liquid nitrogen temperature under impact loading of crept specimen (69 MPa and 1023 K): (*a*) boron-free steel and (*b*) boron-containing steel.

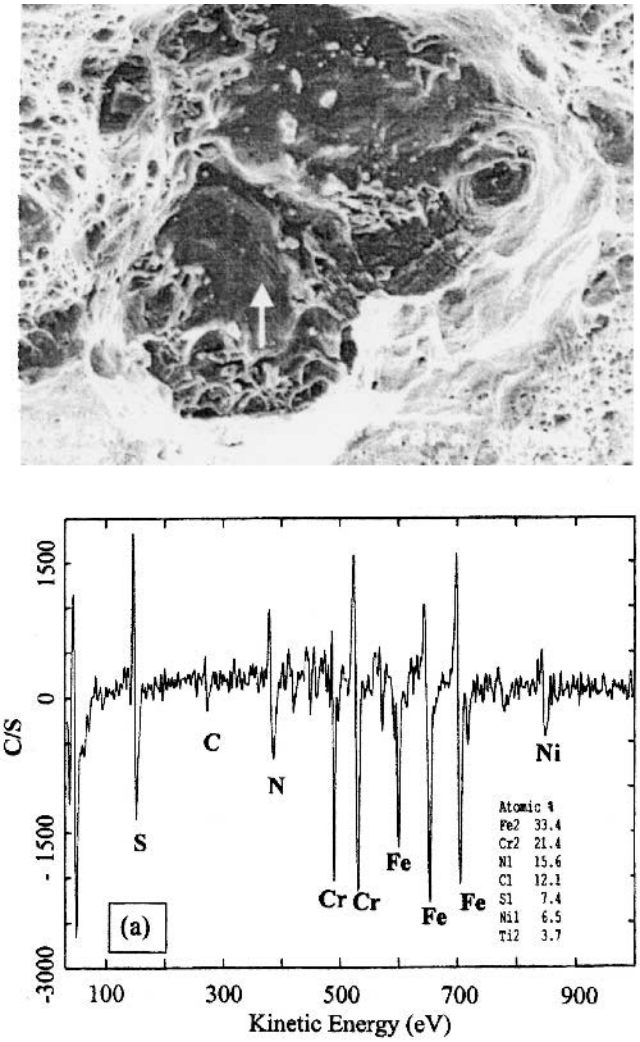

Fig. 22—Auger spectra obtained from a creep cavity surface (indicated) of boron-free steel creep exposed at 69 MPa and 1023 K for 998 h.

because of its relatively high melting point of approximately 2303 K. Therefore, segregation of boron on cavity surfaces provides the steel with the function of self-healing for creep cavitations with an associated increase in creep strength (Figure 3) and ductility (Figures 4 and 5). Since the segregation of boron on the nucleated cavity surface is a diffusion-controlled process, its beneficial effects on creep ductility are revealed better at relatively longer creep exposure times. The increase in creep ductility with creep rupture life (Figures 4, 5, and 8), which is in contradiction to the usual observation of decrease in creep ductility with creep rupture life, may be due to the effects of segregation of boron on creep cavity surfaces. A similar conclusion of self-healing of creep cavitation in a titanium-modified austenitic stainless steel has been reported by Shinya *et al*.[4] However, they reported the filmy precipitation of boron-nitride on the cavity surface. In the present investigation on niobium-stabilized austenitic stainless steel, the relatively stronger affinity of niobium toward nitrogen than that of titanium might have precluded the formation of boron-nitride on cavity surface.

Boron of 0.07 wt pct was added in the steel. This was based on the earlier experience of the self-healing effect for creep cavitation in a type 321 austenitic stainless steel.[4] However, Borland[36] reported that the addition of boron makes the welding of steel more delicate. Decreasing the amount of added boron but still maintaining its self-healing effects for creep rupture strength and ductility is, therefore, desirable in this point of view. Further studies are needed to optimize the boron content in the steel with the function of the self-healing effect for creep cavitation.

IV. CONCLUSIONS

1. Boron addition in type 347 austenitic stainless steel along with cerium greatly increased the creep strength and creep ductility of the steel.
2. Boron addition increased the grain boundary sliding resistance of the steel and suppressed the nucleation and growth of the creep cavity. Enhanced precipitation of carbonitrides and precipitation of borides may be two of the reasons for the increase in grain boundary sliding resistance of the steel with boron addition.
3. Cerium addition was found highly effective in removing even the traces of soluble sulfur in the steel from being deposited on the cavity surface.
4. In the absence of sulfur segregation, filmy segregation of boron on the cavity surface may provide the steel with the function of the self-healing effect of creep cavitations

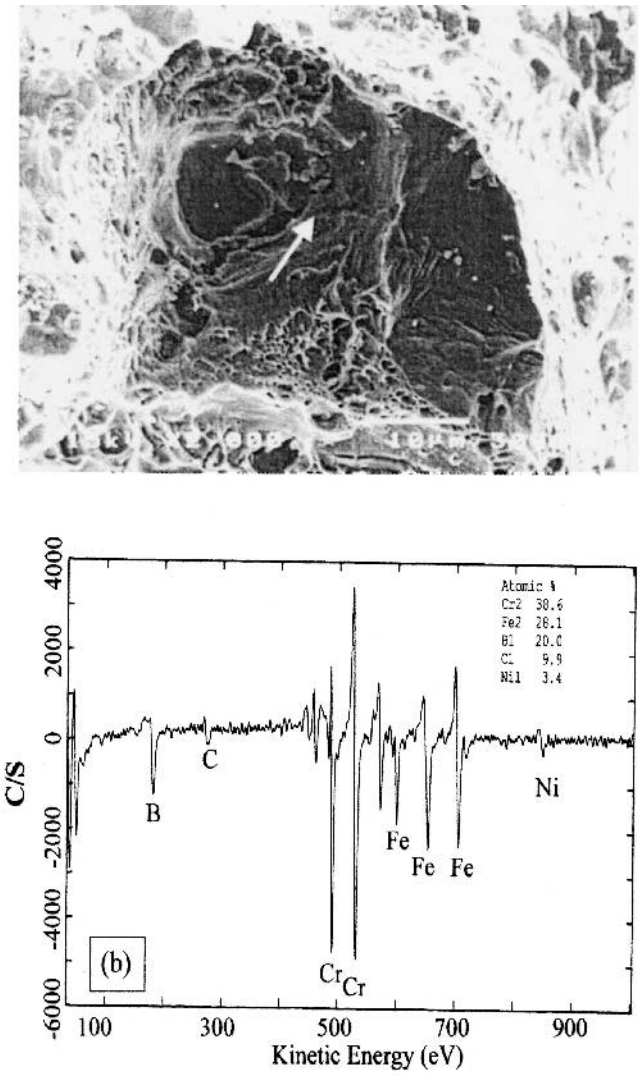

Fig. 23—Auger spectra obtained from a creep cavity surface (indicated) of boron-containing steel creep exposed at 69 MPa and 1023 K for 5461 h.

with the associate increase in creep strength and creep ductility.

ACKNOWLEDGMENTS

One of the authors (KL) gratefully acknowledges the support of the Japanese Society for Promotion of Science (JSPS) for providing the JSPS postdoctoral fellowship for foreign researcher to carry out the research work at the National Institute for Materials Science (Tsukuba, Japan).

REFERENCES

1. T. Ishitsuka and H. Mimura: *Int. Conf. on "Creep and Fatigue at Elevated Temperatures" "Creep 7*," Tsukuba, Japan, June 3–8, 2001, Japan Society of Mechanical Engineers, 2001, pp. 401-06.
2. M. Kikuchi, M. Sakakibara, Y. Otoguro, H. Mimura, T. Takahashi and T. Fujita: *Int. Conf. on "Creep"*, Tokyo, Apr. 14–18, 1986, Japan Society of Mechanical Engineers, 1986, pp. 215-20.
3. Y. Sawaragi and S. Hirano: *The 1990 Pressure Vessels and Piping Conf.*, Nashville, TN, June 17–21, 1990, PVP-vol. 201, MPC-vol. 31, pp. 141-46.
4. N. Shinya, J. Kyono, and K. Laha: *Mater. Sci. Forum*, 2003, vols. 426–432, pp. 1107-12.
5. J. Kallqvist and H.O. Andren: *Mater. Sci. Technol.*, 2000, vol. 16, pp. 1181-85.
6. F. Masuyama: *Int. Conf. on "Advanced Heat Resistant Steel for Power Generation*," San Sebastian, Spain, 1998, R.V. Viswanathan and J. Nutting, eds., pp. 33-48.
7. Y. Minami, H. Kimura, and Y. Ihara: *Mater. Sci. Technol.*, 1986, vol. 2, pp. 795-806.
8. A. Tohyama, M. Miyauchi, and Y. Minami: *Int. Conf. on "Materials for Advanced Power Engineering*," Coutsouradis *et al.*, eds., Kluwer Academic Publishers, 1994, pp. 495-504.
9. H. Trinkaus and H. Ullmaier: *Phil. Mag.*, 1979, vol. 39, pp. 563-80.
10. S.H. Goods and W.D. Nix: *Acta Metall.* 1978, vol. 26, pp. 739-52.
11. J. Perry: *J. Mater. Sci.*, 1974, vol. 9, pp. 1016-39.
12. E.D. Hondros and M.P. Seah: *Int. Met. Rev.*, 1977, vol. 222, pp. 262-301.
13. W.D. Nix, K.S. Yu, and J.S. Wang: *Metall. Trans. A*, 1983, vol. 14A, pp. 563-70.
14. F. Cosandey, D. Li, F. Sczerzenie, and J.K. Tien: *Metall. Trans. A*, 1983, vol. 14A, pp. 611-21.
15. M. Fujiwara, H. Uchida, and S. Ohta: *J. Mater. Sci. Lett.*, 1994, vol. 13, pp. 557-59.
16. H. Teranishi, K. Yoshikawa and Y. Sawaragi: *Int. Conf. on "Creep*," Tokyo, Apr. 14–18, 1986, Japan Society of Mechanical Engineers, 1986, pp. 233-38.
17. T. Sourmail: *Mater. Sci. Technol.*, 2001, vol. 17, pp. 1-14.
18. E.T. Turkdogan: *Proc. Int. Conf. on "Sulfide Inclusions in Steels*," Port Chester, NY, Nov. 7–8, 1974, ASM, Metals Park, OH, J.J. deBarbadillo and E. Snapeeds., 1974, pp. 1-21.
19. H.J. Goldschmidt *J. Iron Steel Inst.*, 1971, vol. 209, pp. 900-09.
20. S.R. Keown and F.B. Pickering: *Int. Conf. on Creep Strength in Steel and High-Temperature Alloys*, The Metal Society, London, University of Sheffield, Sheffield, United Kingdom, 1972, pp. 134-43.
21. R.W. Swindeman and P.J. Maziasz: *Proc. 5th Int. Conf. on "Creep of Materials*," Lake Buena Vista, FL, May 18–21, 1992, ASM INTERNATIONAL, Materials Park, OH, 1992, pp. 33-42.
22. Y.K. Lee, T.Y. Yoo, Y.H. Lee, G. Kim, and S.H. Kwon: *Int. Conf. on "Stainless Steels*," Chiba, Japan, ISIJ, 1991, pp. 905-12.
23. S.R. Keown and F.B. Pickering: *Met. Sci.*, 1977, vol. 11, pp. 225-34.
24. T.M. Williams, D.R. Harries, and J. Furnival: *J. Iron Steel Inst.*, 1972, vol. 210, pp. 351-58.
25. N.G. Needham and T. Gladman: *Met. Sci.*, 1980, vol. 14, pp. 64-72.
26. S. Kishimoto, N. Shinya, and H. Tanaka: *Trans. Nat. Res. Inst. Met., Jpn.*, 1990, vol. 32 (4), pp. 15-19.
27. L. Karlsson and H. Norden: *Acta Metall.*, 1988, vol. 36, pp. 35-48.
28. H.E. Evans: *Mechanisms of Creep Fracture*, Elsevier Applied Science Publishers, London, 1984, pp. 25-65.
29. E. Smith and J.T. Barnby: *Met. Sci. J.*, 1967, vol. 1, pp. 1-5.
30. R.G. Fleck, C.J. Beevers, and D.M.R. Taplin: *Met. Sci.*, 1976, vol. 10, pp. 413-17.
31. H. Tanaka, M. Murata, F. Abe, and K. Yagi: *Mater. Sci. Eng. A*, 1997, vols. 234–236, pp. 1049-52.
32. C.L. White, J.H. Schneibel, and R.A. Padgett: *Metall. Trans. A*, 1983, vol. 14A, pp. 595-610.
33. C.L. White, R.A. Padgett, and R.W. Swindeman: *Scripta Metall.*, 1981, vol. 15, pp. 777-82.
34. M.H. Yoo and H. Trinhaus: *Metall. Trans. A*, 1983, vol. 14A, pp. 547-61.
35. L.E. Davis, M.C. MacDonald, P.W. Palmberg, G.E. Riach, and R.E. Weber: *Hand Book of Auger Electron Spectroscopy*, 2nd ed., Physical Electronics Division, Perkin-Elmer Corporation, MN, 1976.
36. J.C. Borland: *Br. Welding J.*, 1961, vol. 8, pp. 526-40.